Exploding dissipative solitons: The analog of the Ruelle-Takens route for spatially localized solutions

Orazio Descalzi,[1,2,*] Carlos Cartes,[1] Jaime Cisternas,[1] and Helmut R. Brand[2]

[1]*Complex Systems Group, Facultad de Ingeniería y Ciencias Aplicadas, Universidad de los Andes, Av. San Carlos de Apoquindo 2200, Santiago, Chile*

[2]*Department of Physics, University of Bayreuth, D-95440 Bayreuth, Germany*

(Received 7 March 2011; revised manuscript received 22 April 2011; published 25 May 2011)

We investigate the route to exploding dissipative solitons in the complex cubic-quintic Ginzburg-Landau equation, as the bifurcation parameter, the distance from linear onset, is increased. We find for a large class of initial conditions the sequence: stationary localized solutions, oscillatory localized solutions with one frequency, oscillatory localized solutions with two frequencies, and exploding localized solutions. The transition between localized solutions with one and with two frequencies, respectively, is analyzed in detail. It is found to correspond to a forward Hopf bifurcation for these localized solutions as the bifurcation parameter is increased. In addition, we make use of power spectra to characterize all time-dependent states. On the basis of all information available, we conclude that the sequence oscillatory localized solutions with one frequency, oscillatory localized solutions with two frequencies, and exploding dissipative solitons can be interpreted as the analog of the Ruelle-Takens-Newhouse route to chaos for spatially localized solutions.

DOI: 10.1103/PhysRevE.83.056214 PACS number(s): 82.40.Bj, 42.65.Sf, 47.20.Ky, 05.70.Ln

I. INTRODUCTION AND MOTIVATION

Dynamical behavior exhibiting both spatial and temporal disorder is referred to as spatiotemporal chaos [1]. Although much is known about low-dimensional chaos, the knowledge about disordered extended systems consisting of a large number of degrees of freedom and showing chaotic but localized structures is much smaller. In low-dimensional systems three main routes to chaos are well established: period doubling, quasiperiodic or Ruelle-Takens, and intermittency. Following the theoretical work of Ruelle, Takens, and Newhouse [2,3] it had been shown experimentally for Rayleigh-Bénard convection that by increasing the Rayleigh number beyond the appearance of a second frequency chaos sets in [4]. Another example of conversion of quasiperiodic motion into chaotic motion has been found for the Taylor-Couette instability [4]. More recently it has been shown in a combined experimental and numerical study that electroconvection in a thin, sheared film can lead to a transition to localized chaotic convection following the Ruelle-Takens route [5]. In this article we show the analog of the Ruelle-Takens route for spatially localized solutions in a prototype equation, namely the cubic-quintic complex Ginzburg-Landau (CGL) equation. In particular this equation models a passively mode-locked laser operating in a regime in which it produces dissipative exploding solitons [6]. The CGL equation has been derived in different contexts such as binary fluid mixtures, nematic liquid crystals, or chemical reactions since it describes the dynamics of a system at the onset of an oscillatory instability. When coexistence is observed as is the case in binary fluid mixtures (convective state surrounded by conductive state) cubic-quintic CGL equations serve to qualitatively describe localized convective regions and their interactions both in the absence and in the presence of noise [7–9]. The cubic-quintic CGL equation, a dispersive-dissipative system, has stable localized solutions including pulses and holes due to its complex coefficients (which render the equation nonvariational) and quintic nonlinearities. Pulses and holes are either stationary, breathing, chaotic, or moving [10–25]. In the anomalous dispersion regime exploding dissipative solitons have been obtained [6,26–29] and it has been shown that the transition to exploding solitons arises after the appearance of oscillatory localized solutions with two frequencies, as the control parameter (distance from linear onset) is increased [29].

II. THE MODEL

In this article we study the cubic-quintic complex Ginzburg-Landau equation in one spatial dimension. In optics this equation takes the form

$$i\psi_z + \frac{D}{2}\psi_{tt} + |\psi|^2\psi + \nu|\psi|^4\psi = i\delta\psi + i\varepsilon|\psi|^2\psi + i\beta\psi_{tt} + i\mu|\psi|^4\psi. \quad (1)$$

Modeling passively mode-locked lasers Eq. (1) describes the dynamics of the envelope of the electrical field (ψ) in a medium with group velocity dispersion D, linear gain-loss (δ), cubic and quintic nonlinear gain and absorption (ε and μ, respectively), saturation of the nonlinear refractive index (ν), and spectral filtering (β) [6]. Exchanging space and time in the model above ($z \leftrightarrow t$ and $t \leftrightarrow x$) we obtain the cubic-quintic complex Ginzburg-Landau equation for the envelope of the linear unstable modes at the onset of a subcritical oscillatory instability

$$\partial_t A = \mu A + (\beta_r + i\beta_i)|A|^2A + (\gamma_r + i\gamma_i)|A|^4A + (D_r + iD_i)\partial_{xx}A. \quad (2)$$

Along this article we study Eq. (2) for the complex field $A(x,t)$ assuming $\beta_r > 0$ and $\gamma_r < 0$ to have a weakly inverted bifurcation. Our simulations have been carried out in the anomalous dispersion regime ($D_i > 0$) and all parameters have been kept fixed except for μ, which represents the distance from linear onset: $\beta_r = 1$, $\beta_i = 0.8$, $\gamma_r = -0.1$, $\gamma_i = -0.6$, $D_r = 0.125$, $D_i = 0.5$. Table I in [29] can be

*odescalzi@miuandes.cl

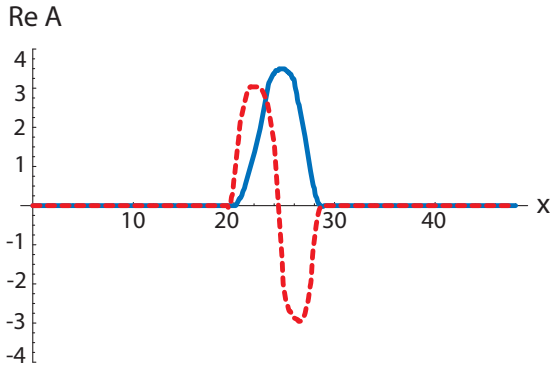

FIG. 1. (Color online) Typical examples of the two classes of initial conditions used: in phase initial conditions (ICP) are shown as a solid line and initial conditions in antiphase (ICA) are shown as a dashed line.

used to compare the coefficients used in Eq. (1) with those in Eq. (2).

In general, results for the above equation depend on the initial conditions, the boundary conditions, and, for anomalous dispersion, weakly on the numerical method used. In this work we used explicit fourth-order Runge-Kutta finite differencing and a time-splitting pseudospectral scheme as independent numerical methods. In both cases we used a grid spacing $dx = 0.08$, a time step $dt = 0.005$, and $N = 625$ so that we get a box size $L = 50$. We note that increasing the accuracy and changing the numerical method the phase diagram might be shifted slightly, but the observed types of behavior are robust. For example, for the pseudospectral method we have for μ_c the value $\mu_c = -0.2316$. In the following asymptotic time regime means $T \approx 2 \times 10^6$ equivalent to 4×10^8 iterations. Nonmoving localized objects are essentially not sensitive to boundary conditions when the box size is large compared to the width of the localized state. In our simulations we have implemented periodic boundary conditions. Initial conditions play an important role in the selection of the outcome when coexistence of solutions is expected. In the present work we use two classes of initial conditions: ICP (initial conditions in phase) and ICA (initial conditions in antiphase) (Fig. 1). The former is obtained by using $\mathrm{Im}A(x) = 0$ and localized $\mathrm{Re}A(x)$ positive (or negative) and the latter by choosing $\mathrm{Im}A(x) = 0$ and $\mathrm{Re}A(x)$ with a positive and a negative part [23].

III. RESULTS

In Fig. 2 we have plotted the behavior we obtain as a function of the control parameter μ. Collapse in Fig. 2 refers to a collapse of all initial data to the zero state and ST refers to the modulus to stationary, that is nonbreathing, localized solutions. To complement our previous paper [29] we focus here on the detailed characterization of two features of the diagram presented in Fig. 2: (a) the transitions of states with one frequency (f_1) to states with two frequencies (f_1, f_2) for both, the asymmetric branch (not in phase) and the symmetric branch (in phase), and (b) the transition to explosions via analysis of the power spectra of the various states.

In Fig. 3 we show snapshots of the modulus $R(x)$ of the states with one frequency f_1 in the asymptotic time regime

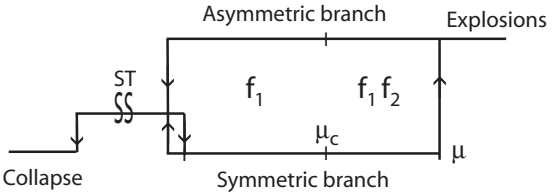

FIG. 2. Phase diagram: the various types of localized states are shown as a function of the bifurcation parameter μ. The other parameters investigated are: $\beta_r = 1, \beta_i = 0.8, \gamma_r = -0.1, \gamma_i = -0.6$, $D_r = 0.125, D_i = 0.5, dx = 0.08$, and $dt = 0.005$. As μ is increased one obtains first stationary pulses (ST), followed by oscillating symmetric pulses with one frequency (f_1) and by a transition to symmetric pulses with two frequencies (f_1, f_2) at μ_c. Denoting by ε the distance from μ_c: $\varepsilon = \mu - \mu_c$, exploding solitons arise stably when μ is increased further beyond $\varepsilon = 1.90 \times 10^{-2}$ until the linear threshold is reached. Reducing the bifurcation parameter μ below $\varepsilon = 1.90 \times 10^{-2}$, exploding solitons are replaced first by asymmetric pulses, that are not in phase, with two frequencies (f_1, f_2), and at $\varepsilon = 0$ a continuous transition to asymmetric pulses (not in phase) with one frequency arises before jumping back to the stationary branch at $\varepsilon = -2.60 \times 10^{-2}$.

for the symmetric, in phase case (a), which can be reached from ICP, as well as for the asymmetric, not in phase branch (b), which can be reached from ICA. In this connection we emphasize that it is important to start with rather precisely symmetric ICPs to obtain the symmetric branch. The notation "in phase" and "not in phase" becomes quite intuitive when inspecting the spatial behavior of the modulus in the wings.

As the bifurcation parameter μ is increased, a transition to a state with two frequencies takes place, which we will now discuss in some detail. In Fig. 4 we show x–t plots in the asymptotic time regime for the two generic cases of states with two frequencies, namely type A and type B. In addition to these generic cases, there are two additional states belonging to the class of states with two frequencies (f_1, f_2), namely the symmetric state with two frequencies oscillating in phase, which has been discussed already in our previous paper ([29], Fig. 4) and the asymmetrically oscillating state, which marks precisely the crossover between states of type A and states of type B. In the latter case the oscillations are staggered at constant time interval left-right-left-right, while for states A and B these time intervals are not equal in duration. All the states described in this paragraph can be reached jumping from a state with one frequency (f_1) or starting with ICP or ICA in the range where two frequencies are expected.

Next we clarify the nature of the transition between the states with one frequency (f_1) and the states with two frequencies (f_1, f_2). To obtain a quantitative characterization we use the ingredients summarized in Fig. 5 for the symmetric branch. Figure 5(a) shows a snapshot of the state on the symmetric branch in the asymptotic time regime. It includes the location x_m for which we have analyzed the time series in detail. Figure 5(b) shows the time series for the in-phase state f_1 with one frequency ω_1 and Fig. 5(c) shows the time series associated with the in-phase state with two frequencies (f_1, f_2) with two vastly different frequencies ω_1 and ω_2. In Fig. 5(c) we have denoted by A_m the peak to peak amplitude of the modulations due to the second frequency ω_2. x_m has

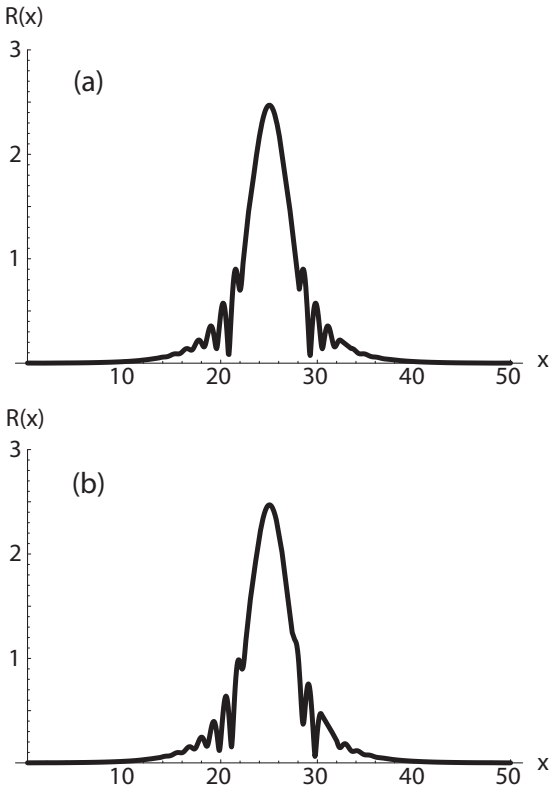

FIG. 3. Snapshot of the the modulus $R(x)$ of the two types of oscillatory states with one frequency (f_1) for $\varepsilon = -3.0 \times 10^{-3}$: (a) symmetric, in phase and (b) asymmetric and not in phase. All other parameters are as in Fig. 2.

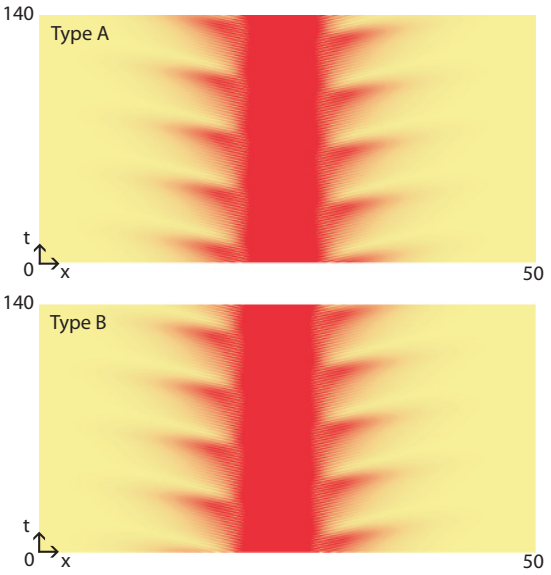

FIG. 4. (Color online) x–t plots for the two generic states (type A and type B) with two frequencies (f_1, f_2) for $\varepsilon = 1.70 \times 10^{-2}$ for a box size $L = 50$ and a time scale $T = 140$ (corresponding to 2.8×10^4 iterations) in the asymptotic time regime. All other parameters are as in Fig. 2.

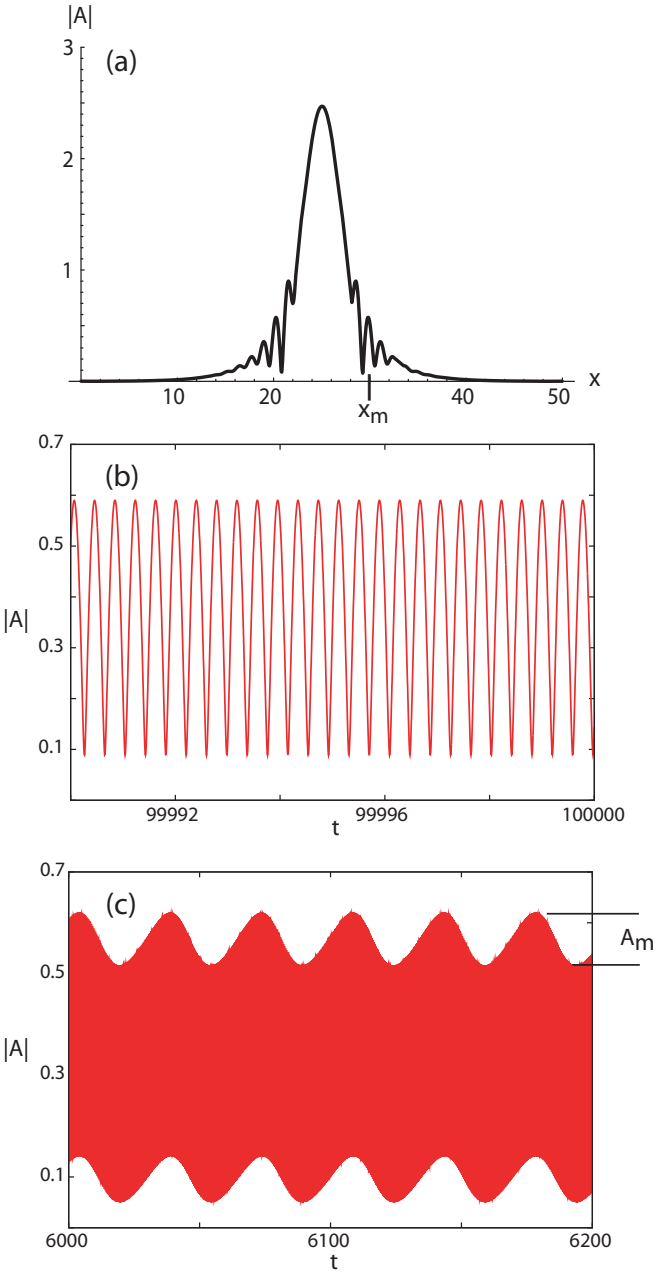

FIG. 5. (Color online) Snapshot and time series for the symmetric branch. (a) Snapshot indicating the location $x_m = 30$ for which the time series are shown. (b) Time series for the in-phase state f_1 with one frequency (ω_1) and $\varepsilon = -10^{-4}$. (c) Time series for the in-phase state with two frequencies f_1, f_2 (with ω_1, ω_2) and $\varepsilon = 1.6 \times 10^{-3}$. All other parameters are as in Fig. 2. Note the vastly different time scale on the abscissa.

been selected to lie in the wings of the states with one or two frequencies, where the time series shown in Figs. 5(b) and 5(c) reveal large effects. Qualitatively there is no change for the time series [shown in Figs. 5(b) and 5(c)] or the power spectra (shown in Fig. 7) for other choices of the location x_m. This is brought out clearly in Fig. 8, where the analog of the power spectra shown in Fig. 7 for the states with one and two frequencies is presented for three different locations, namely for $x_m = 30$ (•), for $x_m = 33$ (dashed line), and for

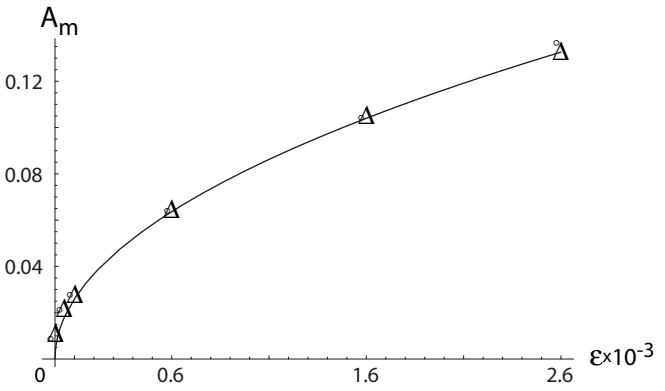

FIG. 6. The modulation amplitude A_m associated with the second frequency is plotted for the symmetric branch (○) as well as for the asymmetric branch (△). The solid line is a fit to the data of the form $A_m = A_{m_0}\sqrt{\varepsilon}$ with $A_{m_0} = 2.60$. This plot demonstrates that all our data are compatible with a secondary Hopf bifurcation characterized by the second frequency ω_2.

$x_m = 36$ (▲). Thus while the amplitudes of the peaks in the power spectra change, their location remains the same.

In Fig. 6 we have plotted for both the symmetric branch (△) and the asymmetric branch (○) the modulation amplitude A_m introduced above as a function of ε. The solid line represents a fit to all data points (the symmetric and the asymmetric branch are fitted simultaneously). Since we find $A_m^2 \sim \varepsilon$, we conclude that the transition from the one frequency state f_1 to the two frequency state f_1, f_2 is a forward Hopf bifurcation. This conclusion is also consistent with all our numerical results showing absolutely no indication of any hysteresis effect associated with this transition.

To analyze the transition to explosions and their complex spatiotemporal behavior, we have investigated the power spectrum for the explosive dissipative soliton state as well as for the two preceding oscillatory states at lower values of the bifurcation parameter μ. In Figs. 7 and 8 we have plotted the corresponding results. For the one frequency state f_1 we conclude immediately from the power spectrum that we have indeed only one frequency ω_1 along with its harmonics. Increasing the bifurcation parameter we crossover to the two frequency state f_1, f_2 analyzed above. From the power spectrum shown in Fig. 7(b) we conclude (as already from the corresponding x–t plots) that the two frequencies ω_1 and ω_2 are vastly different. To demonstrate the presence of higher harmonics for the second, much lower frequency, we show as an inset in Fig. 7(b) the low-frequency behavior on a logarithmic scale revealing the presence of a second harmonic also for the second frequency. Analyzing the data quantitatively, we find for the ratio between the two frequencies $\omega_1/\omega_2 \approx 89.8$. As the bifurcation parameter μ is increased further and reaches the domain of explosive solitons, we obtain the power spectrum shown in Fig. 7(c). Figure 7(c) closely resembles results for low-dimensional chaotic systems such as ordinary differential equations and maps. As a rather characteristic feature one gets broad band low-frequency noise. In addition, we see the remnant of the peak for the large frequency ω_1.

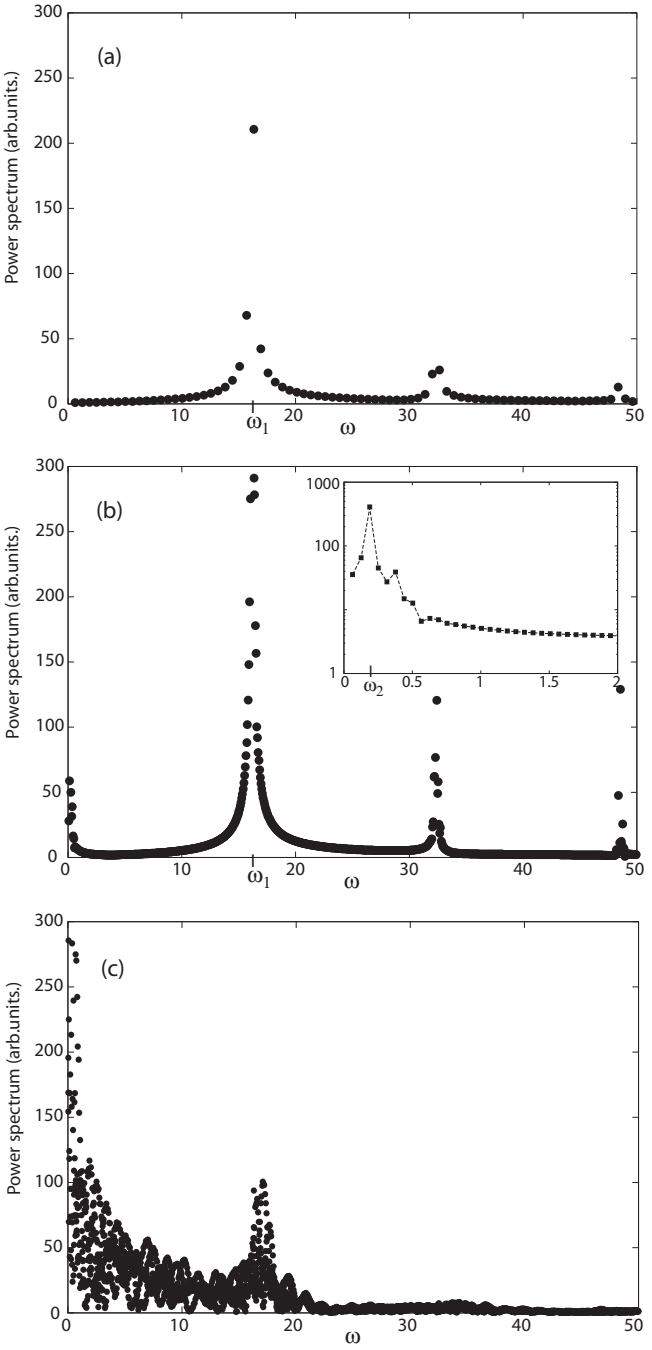

FIG. 7. The power spectrum is plotted as a function of ε for $x_m = 30$. (a) $\varepsilon = -10^{-4}$, only one frequency ω_1 and its harmonics are present in the power spectrum. (b) $\varepsilon = 1.6 \times 10^{-3}$, two frequencies ω_1 and ω_2 and their harmonics are present in the power spectrum. The inset shows the higher harmonics of ω_2, the ratio ω_1/ω_2 takes the value $\omega_1/\omega_2 \approx 89.8$. (c) For $\varepsilon = 1.86 \times 10^{-2}$ the power spectrum shows features characteristic of chaos including its characteristic low-frequency behavior. Inspection of (c) shows the remnant of the peak for frequency ω_1. All other parameters are as for Fig. 2.

IV. SIMILARITIES/ANALOGIES TO THE RUELLE-TAKENS-NEWHOUSE SCENARIO

Thus we obtain for the localized states, which are stable solutions of a partial differential equation with dissipation and

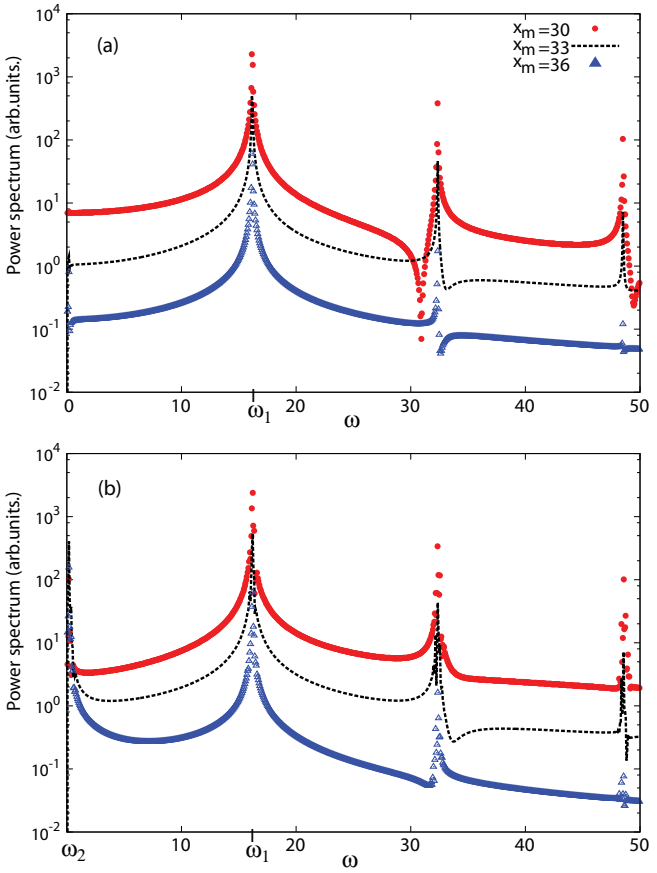

FIG. 8. (Color online) The power spectrum is plotted for the states with one and with two frequencies as a function of the location x_m: $x_m = 30$ (•), $x_m = 33$ (dashed line), and $x_m = 36$ (▲). (a) $\varepsilon = -10^{-4}$, only one frequency ω_1 and its harmonics are present in the power spectrum. (b) $\varepsilon = 1.6 \times 10^{-3}$, two frequencies ω_1 and ω_2 and their harmonics are present in the power spectrum. We note that the scale on the ordinate is logarithmic in this figure in contrast to Fig. 7. All other parameters are as for Fig. 2.

dispersion, the following route: one frequency, two frequencies, and then chaotic behavior as the bifurcation parameter μ is increased. This indicates that we have in a spatially extended system for localized states a rather close analog of the Ruelle-Takens-Newhouse scenario for the route to chaotic behavior [2,3] (cf., e.g., Refs. [30,31] for further details of the Ruelle-Takens-Newhouse scenario), here in the sense of spatiotemporally disordered behavior in terms of exploding solitons. Here the state with two frequencies is the analog of the two torus in the low-dimensional system, which breaks down giving rise to the spatiotemporal behavior characteristic of explosive dissipative solitons. We did not observe a third frequency, a situation which is one of the generic cases according to Ref. [3]. We also note that in the present system one does not expect any universal scaling behavior of the nature found for maps near the transition from a two torus to chaotic behavior, since the ratio of the two frequencies revealed by our system is far away from the golden mean.

We note that the physical picture for the spatial aspects of the transition from the state with one frequency to the explosive dissipative soliton via the state with two frequencies has been described in detail in [29]. Coming from the state with one frequency, for the state with two frequencies the amplitude of the wings increases. Further increasing the bifurcation parameter, the maximum amplitude in the wings overcomes a certain threshold value, which allows a second peak to grow, which then interacts in turn with the main peak leading to a further growth and the fusion with the main peak before the whole object collapses due to its inherent instability [29].

V. CONCLUSIONS AND PERSPECTIVE

In this paper we have analyzed the bifurcation sequence from stationary localized solutions to spatially localized exploding dissipative solitons for a large class of initial conditions as a function of the bifurcation parameter for the complex cubic-quintic Ginzburg-Landau equation in the regime of anomalous linear dispersion. This equation is a prototype envelope equation arising for weakly subcritical transitions to traveling and standing waves. Two main results emerge from our study.

First we have shown that the bifurcation from localized oscillatory states with one frequency to localized oscillatory states with two frequencies is a forward Hopf bifurcation without any hysteresis. Analyzing the whole sequence from stationary localized states to exploding dissipative solitons by various techniques including power spectra for all time-dependent states, we find the analog of the Ruelle-Takens-Newhouse route to chaos for spatially localized solutions in a spatially extended system characterized by a prototype envelope equation: the cubic-quintic complex Ginzburg-Landau equation.

Naturally the question of the connection of the results presented here to experimentally accessible systems arises. While exploding dissipative solitons have been observed experimentally in a nonlinear optical system [6], the analog of the bifurcation parameter has not been varied systematically in these experiments to investigate the sequence of transitions studied here. Nevertheless, clearly a nonlinear optical system of the type studied by Cundiff *et al.* [6] is a prime candidate to check the predictions made here.

We also note, as already discussed above briefly, that the analog of the Ruelle-Takens-Newhouse scenario for spatially localized states has been observed experimentally in sheared electroconvection recently [5]. However, this system showed strongly subcritical behavior. In addition, it would be worthwhile to check to what extent the spatially localized chaotic states reported in Ref. [5] are similar in nature to exploding dissipative solitons [6,26–29] or whether they are more closely related to the chaotic localized states found for the complex cubic-quintic Ginzburg-Landau equation in the regime of normal linear dispersion [19,32,33]. It would also be very interesting to investigate whether the parameters for sheared electroconvection could be tuned in such a way to render the basic transition weakly subcritical instead of strongly hysteretic.

ACKNOWLEDGMENTS

O.D. acknowledges the Deutsche Akademische Austauschdienst for financial support during his stay at the University of Bayreuth. O.D., C.C., and J.C. wish to thank the support of FONDECYT (Projects No. 1110360 and No. 3110028) and

Universidad de los Andes through FAI initiatives. H.R.B. thanks the Deutsche Forschungsgemeinschaft for partial support of this work through the Forschergruppe FOR 608. 'Nichtlineare Dynamik komplexer Kontinua.'

[1] M. C. Cross and P. C. Hohenberg, Rev. Mod. Phys. **65**, 851 (1993).
[2] D. Ruelle and F. Takens, Commun. Math. Phys. **20**, 167 (1971); **23**, 343 (1971).
[3] S. Newhouse, D. Ruelle, and F. Takens, Commun. Math. Phys. **64**, 35 (1978).
[4] H. L. Swinney and J. P. Gollub, Phys. Today **31**(8), 41 (1978).
[5] P. Tsai, S. W. Morris, and Z. A. Daya, Europhys. Lett. **84**, 14003 (2008).
[6] S. T. Cundiff, J. M. Soto-Crespo, and N. Akhmediev, Phys. Rev. Lett. **88**, 073903 (2002).
[7] P. Kolodner, Phys. Rev. A **44**, 6448 (1991).
[8] P. Kolodner, Phys. Rev. A **44**, 6466 (1991).
[9] O. Descalzi, J. Cisternas, D. Escaff, and H. R. Brand, Phys. Rev. Lett. **102**, 188302 (2009).
[10] O. Thual and S. Fauve, J. Phys. (France) **49**, 1829 (1988).
[11] H. R. Brand and R. J. Deissler, Phys. Rev. Lett. **63**, 2801 (1989).
[12] R. J. Deissler and H. R. Brand, Phys. Lett. A **146**, 252 (1990).
[13] S. Fauve and O. Thual, Phys. Rev. Lett. **64**, 282 (1990).
[14] W. van Saarloos and P. C. Hohenberg, Phys. Rev. Lett. **64**, 749 (1990).
[15] V. Hakim and Y. Pomeau, Eur. J. Mech. B/Fluids **10**, 137 (1991).
[16] R. J. Deissler and H. R. Brand, Phys. Rev. A **44**, R3411 (1991).
[17] H. Sakaguchi, Prog. Theor. Phys. **86**, 7 (1991).
[18] H. Sakaguchi, Prog. Theor. Phys. **89**, 1123 (1993).
[19] R. J. Deissler and H. R. Brand, Phys. Rev. Lett. **72**, 478 (1994).
[20] N. Akhmediev, J. M. Soto-Crespo, and G. Town, Phys. Rev. E **63**, 056602 (2001).
[21] O. Descalzi, S. Martinez, and E. Tirapegui, Chaos Solitons Fractals **12**, 2619 (2001).
[22] O. Descalzi, M. Argentina, and E. Tirapegui, Int. J. Bifurcation Chaos Appl. Sci. Eng. **12**, 2459 (2002); Phys. Rev. E **67**, 015601(R) (2003).
[23] O. Descalzi and H. R. Brand, Phys. Rev. E **72**, 055202(R) (2005).
[24] O. Descalzi, H. R. Brand, and J. Cisternas, Physica A **371**, 41 (2006).
[25] P. Gutiérrez, D. Escaff, S. Pérez-Oyarzún, and O. Descalzi, Phys. Rev. E **80**, 037202 (2009).
[26] J. M. Soto-Crespo, N. Akhmediev, and A. Ankiewicz, Phys. Rev. Lett. **85**, 2937 (2000).
[27] N. Akhmediev and J. M. Soto-Crespo, Phys. Lett. A **317**, 287 (2003).
[28] N. Akhmediev and J. M. Soto-Crespo, Phys. Rev. E **70**, 036613 (2004).
[29] O. Descalzi and H. R. Brand, Phys. Rev. E **82**, 026203 (2010).
[30] P. Bergé, Y. Pomeau, and C. Vidal, *Order Within Chaos: Towards a Deterministic Approach to Turbulence* (Wiley, New York, 1986), Chap. VII.2.
[31] M. C. Cross, [http://crossgroup.caltech.edu/ChaosCourse], Chap. 21.
[32] R. J. Deissler and H. R. Brand, Phys. Rev. Lett. **74**, 4847 (1995).
[33] R. J. Deissler and H. R. Brand, Phys. Rev. Lett. **81**, 3856 (1998).